Presented at the 35th PVSC, June 20-25, 2010, Honolulu, Hawaii

COMPARISON OF INTRINSIC AMORPHOUS SILICON BUFFER LAYERS FOR SILICON HETEROJUNCTION SOLAR CELLS DEPOSITED WITH DIFFERENT PECVD TECHNIQUES

D. Pysch, C. Meinhardt, K.-U. Ritzau, M. Bivour, K. Zimmermann, C. Schetter, M. Hermle, S. W. Glunz
Fraunhofer Institute for Solar Energy Systems, Heidenhofstr. 2, 79110 Freiburg, Germany
e-mail: damian.pysch@ise.fraunhofer.de

ABSTRACT

In this investigation we compare intrinsic hydrogen diluted amorphous a-Si:H(i) layers deposited by inductively coupled plasma (ICP) to the standard parallel plate (PP) plasma, driven by 13.5 MHz power source. We analyze and compare the growth rate, optical energy gap, homogeneity, passivation quality, and most importantly silicon heterojunction solar cell performance. The ICP a-Si:H(i) layer shows superior properties regarding the growth rate, however, we obtain a slightly better passivation quality with the PP a-Si:H(i) layer, with V_{oc} values up to 723 mV. Looking at the overall solar cell performance we were not able to see any difference between ICP and PP silicon heterojunction solar cell. The best solar cell (with an ICP a-Si:H(i) layer) has an efficiency of 18.7%.

INTRODUCTION

Silicon Heterojunction (SHJ) solar cells have attracted an increasing interest in the past few years [1-8]. The combination of a very short and low temperature process of the solar cells together with very high efficiency η and open-circuit voltage V_{oc} potential make this solar cell design interesting for research and industry. However, very high V_{oc} and η values have only been show for SHJ solar cells including a thin intrinsic amorphous a-Si:H(i) interface layer [9, 10]. S. Taira *et al.* [11] stated that it is tremendously important to have good surface clean and a soft deposition of the a-Si:H(i) to produce high V_{oc} and η. In this investigation we will focus on two different techniques to deposit the a-Si:H(i) layer: (i) the well known and widely spread parallel plate PP PECVD set-up driven by a 13.5 MHz power source, and (ii) the inductively coupled plasma ICP PECVD setup. It was already shown that both PECVD techniques perform very well regarding their passivation quality of ultra thin ($d_{a\text{-}Si}$<10nm) a-Si:H(i) layer [12]. In the following investigation will compare the a-Si:H(i) layers deposited by ICP (remote, soft plasma) to the PP (direct Plasma) regarding growth rate, optical energy gap, homogeneity, passivation quality, and most important SHJ solar cell performance.

EXPERIMENTAL

Thickness, and optical band gap of the a-Si:H layers were determined by spectroscopic ellipsometry. All measurements shown were performed using a J.A. Woolam C. VASE rotating analyzer ellipsometer. The angle of incidence was 70° and a Tauc-Lorentz-model was used to fit the data [13]. SunsVoc measurements were performed with a SunsVoc measurement setup by Sinton Consulting [14]. The passivation quality and performance of the SHJ solar cells was analyzed on 4 inch, *n*-type,1 Ω cm, FZ silicon wafers with a thickness of 210µm. The solar cell process was the following: a 200nm SiO_2 were thermally grown on the front and back side of the wafer. Next we created an inverted pyramid surface on five out the seven solar cell areas on the front side. Seven 2x2 cm^2 cell areas were defined by photolithography on the front side. The SiO_2 was removed in a HF solution. Prior to the deposition of the a-Si:H(i,p) and Si:H(i,n) stacks on the front and back side, respectively, the wafer were cleaned wet-chemically by a simple oxidization in HNO_3 followed by a removal of the grown oxide in NH_4F [15, 16]. In order to guarantee a sufficient lateral conductivity and to improve the optical properties on the back side, ITO was deposited by magnetron sputtering on both sides. The actual rear metal contact was created by thermal evaporation of titanium Ti (50nm), palladium Pd (50nm), and 1.5 µm of silver Ag. The front side seed layer contact grids were defined by means of photolithography and thermal evaporation of Ti(50 nm), Pd (50nm), and Ag (100nm). Finally, the seed layer was thickened by light-induced plating of silver [17] to obtain a sufficient contact height of 5-10 µm. The a-Si:H(i,n,p), and ITO layers were all deposited using a “System 100 Pro”, a multi PECVD chamber cluster tool by Oxford Instruments.

Parallel Plate Plasma

In a parallel plate plasma deposition the reactive gases (e.g. silane and hydrogen) are injected directly between the parallel plates. In our configuration the upper electrode is connected to an external power source with an alternating potential with a frequency of (in most cases) 13.5 MHz. The lower electrode is grounded. The wafer or substrate is mostly placed on the lower electrode (see Fig. 1). This deposition technique includes a direct interaction between the wafer and the energetic particles generated in the plasma [18, 19].

Inductive Coupled Plasma

In an inductively coupled plasma deposition a tube is placed in the center of a coil which is connected to an

external power source with an alternating potential with a frequency of 13.5 MHz (see Fig. 1). Argon is streaming through the tube from the top. Once the external power source is on, an argon plasma is generated in the center of the tube. The down stream of the argon causes also a downstream of the argon plasma. The actual reactive gases are added to the plasma in the reaction chamber between the tube and substrate electrode. The distance between the plasma tube and the wafer can be varied. The impact of high energetic particles in the plasma on the wafer can be influenced by this distance between the wafer and the ICP plasma tube [20-22].

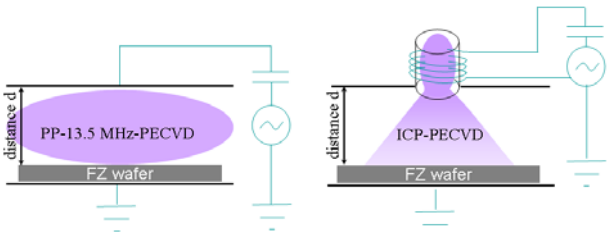

Figure 1 Sketch of a parallel plate (PP) PECVD setup (left side) and a inductively coupled plasma (ICP) setup (right side).

RESULTS

Growth rate of amorphous silicon

In Figure 2 the dependence of the deposited a-Si:H layer thickness on the deposition time is shown. The deposition time t_{depo} defines the time while the actual deposition takes place and plasma is ignited. The growth of a-Si:H can divided in two regimes: (i) the fast initial growth $g_{initial}$ (t_{depo}<10sec), and (ii) the stable, linearly time-dependent growth g_{stable} (t_{depo}>10sec). A measure for $g_{initial}$ of a-Si:H is the intercept of a linear fit to the stable growth grime. A measure for the stable growth rate is the slope of the linear fit of Figure 2. The intrinsic a-Si:H layers under investigation show a good passivation quality [12] and will be applied for a SHJ solar cell process later on in this publication.

Figure 2 illustrates that it is very difficult to deposit an a-Si:H layer thickness below 5 nm with the parallel (PP) set up in a reproducible way. During this process the PECVD chamber is filled with process gases until the process pressure is reached and then the plasma is ignited. Due to this procedure and due to the direct plasma between the parallel plates we observe a very high initial growth rate within the first 5 seconds $g_{initial,PP}$=3.5 to 3.9 nm. The inductively coupled plasma (ICP) shows a much smaller initial growth $g_{initial,ICP}$=0.4 nm. However the stable growth rate is comparable for ICP and PP deposition, 1.1 and 1.6 Å/s, respectively. Thus, the main difference regarding the deposition of a-Si:H between PP and ICP a-Si:H deposition is the much lower initial growth rate of the ICP PECVD.

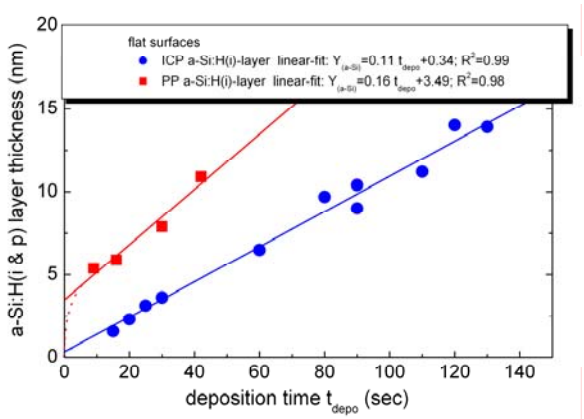

Figure 2 Comparison of the dependence of the a-Si:H layer thickness on the deposition time for PP and the ICP deposition technique. Dotted lines are guides to the eye.

One possible reason for this observation is the much softer and remote plasma applied during ICP deposition. Another reason for the low initial growth rate is, that in our ICP a-Si:H process, the PECVD chamber is filled with nitrogen until the process pressure is reached. The ignition of the plasma and injection of the process gases takes place simultaneously. Thus, at the very beginning of our actual deposition process (t_{depo}=0 sec) there are no process gases in the PECVD chamber. Therefore, our a-Si:H which is deposited within the first 5 to 10 sec contains an unknown amount of silicon nitride.

Dependence of the optical band gap on the a-Si:H thickness

We have investigated the dependence of the optical band gap $E_{g,optical}$ (measured by spectral ellipsometry, Tauc-Lorentz-model) on the a-Si:H(i) layer thickness $d_{a\text{-}Si}$ (see Fig.3).

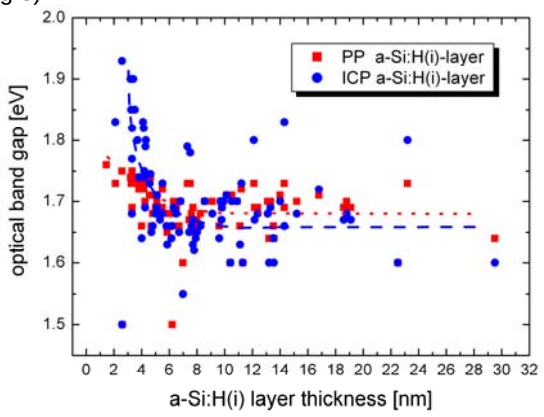

Figure 3 Comparison of the dependence of the optical band gap on the deposited a-Si:H(i) layer thickness. The a-Si:H(i) layer was deposition by the PP and the ICP deposition technique. Optical band gap and thickness measurements were performed by spectral ellipsometry. Dotted lines are guides to the eye.

The PP a-Si:H(i) layers show a constant $E_{g,optical}$ for d_{aSi}>5 nm of $E_{g,optical,PP}$=1.69±0.08 eV. The ICP a-Si:H(i) layers show the same behavior, a constant $E_{g,optical}$ for d_{aSi}>5 nm of $E_{g,optical,ICP}$=1.66±0.08 eV. For a a-Si:H(i) layer thickness $d_{a\text{-}Si}$ <5 nm we examine a significant difference: $E_{g,optical,PP}$=1.68±0.13 eV, and $E_{g,optical,ICP}$=1.75± 0.12 eV. Both a-Si:H(i) layers show a trend to higher $E_{g,optical}$ values with a decrease of $d_{a\text{-}S}$ below 5 nm. However, this trend is much stronger for the ICP a-Si:H(i) layers. This, observation can be explained by the build-in of nitride during first second of the ICP a-Si:H(i) layer deposition.

Radial homogeneity of deposited a-Si:H

The diameter of the ICP tube is only 65mm (2.65 inch). Since we aim for depositing high quality a-Si:H(i) layers on a 102 mm (4 inch) or bigger wafer it is important to check the radial homogeneity of our process. Figure 4 shows the normalized a-Si:H(i) layer thickness for five different sample distances between the ICP plasma tube and the sample. The homogeneity of the samples processed with a distance of 120 to 140 mm is satisfying. A reduction of the distance below 120mm leads to a strong inhomogeneity. This can be most likely overcome by a bigger diameter of the ICP tube.

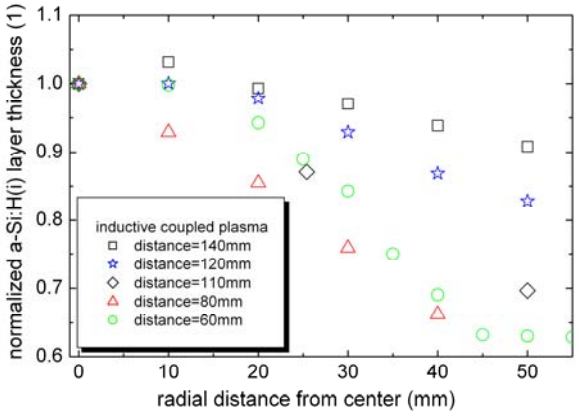

Figure 4 Radial decrease of the normalized a-Si:H layer thickness. The a-Si:H(i) layer was deposited on a 6 inch flat FZ wafer by ICP-PECVD with a variation of the distance of between plasma source and sample (see Fig 1). Thickness measurements were performed by spectral ellipsometry.

The same measurements have been performed to check the homogeneity of the PP a-Si:H(i) layer thickness. Figure 5 shows that the homogeneity is independence of the distance between the electrodes of the parallel plate; every process provides good homogeneity.

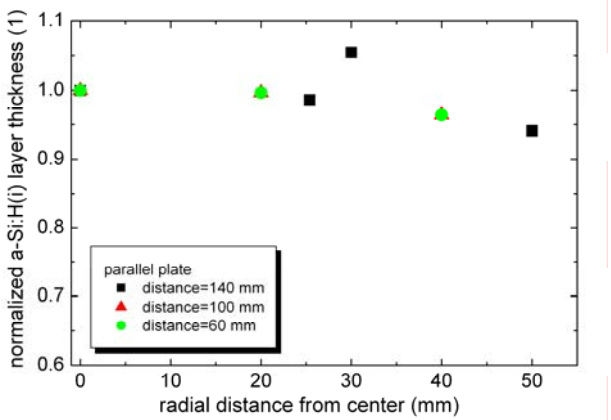

Figure 5 Radial decrease of the normalized a-Si:H layer thickness. The a-Si:H(i) layer was deposited on a 6 inch flat FZ wafer by PP-PECVD with a variation of the distance of between plasma source and sample (see Fig 1). Thickness measurements were performed by spectral ellipsometry.

***V_{oc}* dependence on the a-Si:H(i) layer thickness**

We applied the a-Si:H(i) layers that have been investigated regarding their growth rate, $E_{g,optical}$, and homogeneity to a solar cell process. In Figure 6 & 7 the dependence of SunsV_{oc} measurement on the a-Si:H(i) layer thickness (ICP and PP) is shown for a flat and a textured (inverted pyramids) front surface. We performed the SunsV_{oc} measurements prior to the silver plating process of the front contact. For the flat front surface the V_{oc} values increase with the a-Si:H(i) layer thickness. The V_{oc} values saturate at a layer thickness around 9 nm. A very high V_{oc} saturation level of 720 mV for the PP and 715 mV for ICP a-Si:H(i) layer can be reached.

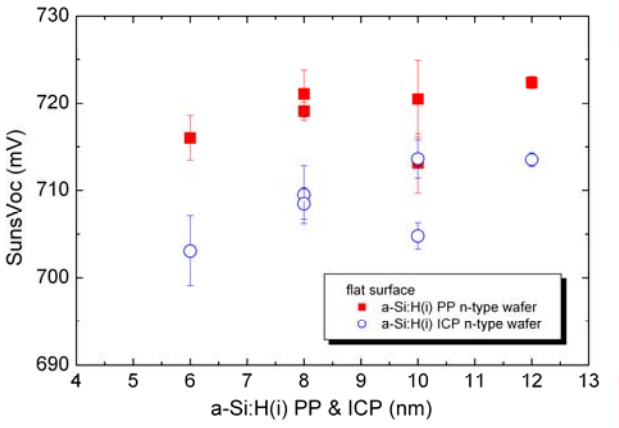

Figure 6 Measurements of the dependence of the open-circuit voltage on the thickness of a-Si:H(i) layer by a SunsVoc measurement setup of fully proceed heterojunction solar cells with a flat front surface. The a-Si:H(i) layer was deposited by the ICP and PP PECVD technique.

For the textured front surface solar cells we observe a very similar behavior (see Fig. 7). However, the saturation level of the V_{oc} is shifted to lower values of 710 mV for the PP and 690 mV for ICP a-Si:H(i) layers. The saturation point regarding the a-Si:H(i) layer thickness is also shifted to higher values ($d_{a\text{-}Si,PP}$=10nm and $d_{a\text{-}Si,ICP}$=12 nm). The main reason for this shift of the saturation point to a higher a-Si:H(i) layer thickness is the decreased a-Si:H(i) layer thickness on a textured compared to a flat surface. The a-Si:H(i) layer thickness on a textured surface can not be measured by the spectral ellipsometry set-up we used. Since the textured and flat solar cells are placed on the same 4 inch wafer we measured the a-Si:H(i) layer thickness on the flat font surface and plotted both V_{oc} (Fig. 6 & 7) values over the same (flat front surface) a-Si:H(i) layer thickness. To get an approximated value of the a-Si:H(i) layer thickness on a textured surface we need to divide the a-Si:H(i) layer thickness measured on a flat front surface by an empirical factor of 1.5 [3, 5]. Applying this assumption to a-Si:H(i) layer thicknesses of Figure 7, the saturation point of the flat and texture surface would be approximately in the same range. This observation gives a hint that there is no strong negative influence of the different crystallographic orientations caused by surface texturing on the passivation quality and thus on the V_{oc} values for the solar cells under investigation. The decrease is probably mainly caused by the reduction of the a-Si:H(i) layer thickness as well as the increase of the total surface area due to the surface texture.

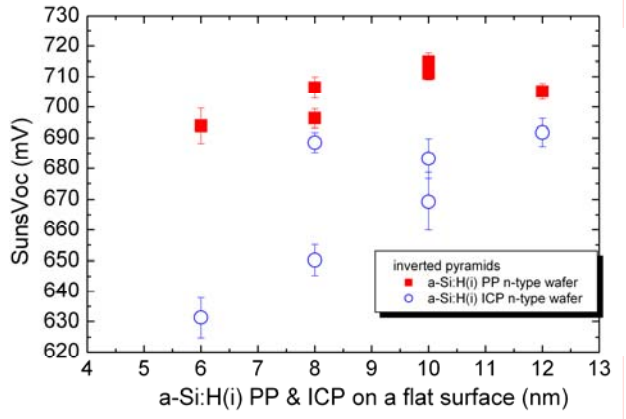

Figure 7 Measurements of the dependence of the open circuit voltage on the thickness of a-Si:H(i) layer by a SunsVoc measurement setup of fully processed heterojunction solar cells with a textured (inverted pyramids) front surface. The a-Si:H(i) layer was deposited by the ICP and PP PECVD technique.

Solar cell results

The SHJ solar cells were processed as described in the experimental chapter above. In Figure 8 the dependence of short- circuit current density J_{sc}, V_{oc}, fill factor *FF*, and η on the PP a-Si:H(i) (x-axis) and a-Si:H(p) layer thickness (parameter in Fig. 8) deposited on a textured front surface are shown. As expected J_{sc} is decreasing with increasing a-Si:H(i) and a-Si:H(p) layer thickness. The opposite dependence is observed for V_{oc}. With increasing a-Si:H(i) and a-Si:H(p) layer thickness V_{oc} rises. The fill factors are in the range between 68 and 75% and show no clear dependence neither on a-Si:H(i) nor on the a-Si:H(p) layer thickness. This observation was not expected. An increasing a-Si:H(i) layer thickness, with a high resistivity should reduce the *FF*. The most likely explanation for the low and uncorrelated *FF* values are technological problems with the front side metallization. Despite, this obvious FF problems an efficiency of 18.7% was achieved with a 9 nm ICP a-Si:H(i) and a 9 nm a-Si:H(p) layer thickness. Thus, the overall a-Si:H-layer thickness on flat surface accounts 18nm for the best solar cell. Since, we deposited this a-Si:H-layer stack on a inverted pyramid surface we assume the real a-Si:H-layer stack thickness to be 12 nm (using the empirical factor of 1.5).

The same variation of the a-Si:H(i) and a-Si:H(p) layer thickness was performed with a-Si:H(i) layers deposited by the PP plasma setup. The obtained results are very similar to the shown in Figure 8.

Figure 9 summarizes the IV parameter results of Figure 8 (ICP a-Si:H(i)) and of the PP a-Si:H(i) layer thickness variation (not shown here). The overall solar cells averaged, the standard deviations, as well as the best values for each parameter are shown. Additionally, an average value of the total a-Si:H layer thickness is shown to guarantee the comparability of the data.

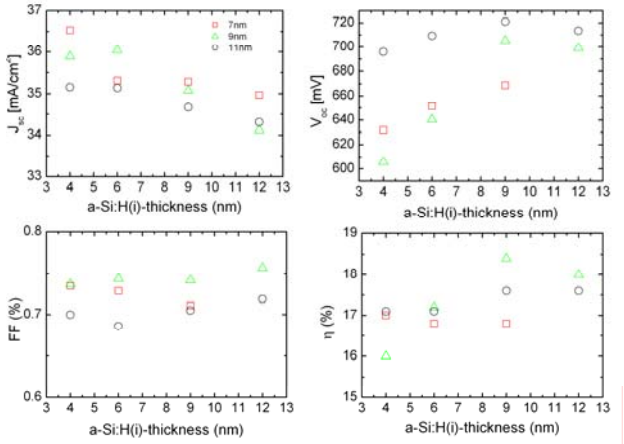

Figure 8 Measurements of the dependence of the *IV*-parameter J_{sc}, V_{oc}, *FF*, and η of a textured FZ silicon *n*-type wafer full heterojunction solar cells on the a-Si:H(i) and a-Si:H(p) layer thickness. The a-Si:H(p) layer was deposited by PP-PECVD. The a-Si:H(i) layer was deposited by PP-PECVD technique.

The only obvious difference in Figure 9 is the slightly higher V_{oc} for the a-Si:H(i) layer deposited by the PP plasma setup. For all other parameter no differences can be distinguished. The best solar cell produced with a PP a-Si:H(i) layer is η_{PP}=18.6% and η_{ICP}=18.7% for the ICP a-Si:H(i) layer.

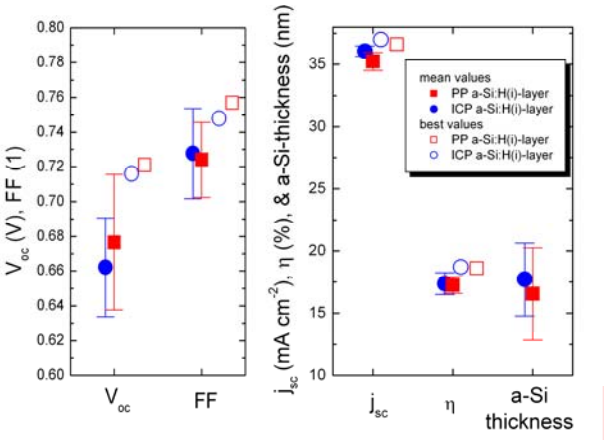

Figure 9 Average and standard deviation error values of the V_{oc}, J_{sc}, *FF*, η and total a-Si:H layer thickness shown in Figure 8 (closed symbols). The best values for each IV parameter are shown by open symbols.

DISCUSSION

In this chapter we will summarize the pros and cons of each a-Si:H(i) deposition technique applied for SHJ solar cells.

As long as one can assure a good passivation quality it is important to be able to deposit a-Si:H layer thicknesses of e.g. 5 nm and even thinner with a high quality and reproducibility. Since, the ICP technique shows a lower initial as well as stable growth rate, the ICP performs better than the PP deposition technique regarding this aspect. The homogeneity of the PP a-Si:H(i) layer is by far better compared with the ICP layer. However, increasing the distance between the ICP-tube and the sample helps. A bigger diameter of the ICP-tube may also help to overcome the homogeneity problem.

We observe a higher optical band gap for the ICP deposited a-Si:H(i) layers, due to the different gasses used (N_2 for ICP and process gases for PP) to flood the PECVD chamber prior to the deposition. On the one hand this is a good finding, since, a higher $E_{G,optical}$ means a lower light absorption in the highly recombinative a-Si:H(i) layer. On the other hand it is know that an increase in the N_2 content in the a-Si:H layer or a increase in $E_{G,optical}$ reduces the conductivity of the layer and can lead to FF problems [23, 24]. Unfortunately, we haven't be able to see any FF differences between the PP and ICP a-Si:(i) layer. To clarify the question whether there is a negative influence of the N_2 in the ICP a-Si:(i) layer on the FF the experiment needs to be repeated with assuring a very low series resistance input of all other series resistance contributors.

The passivation quality of the PP a-Si:(i) layer is slightly better. However, this advantage is not observable in the solar cell efficiency. In general, we must say that a passivation quality on such a high level is very much depended on the actual conditions of PECVD chamber which can vary from day to day and are not easy to control.

CONCLUSION

We showed in this investigation that a-Si:H(i) layers deposited by ICP PECVD technology have a low initial, and stable growth rate, an increased optical band gap for an a-Si:H(i) layer thickness below 5 nm, a poor homogeneity for a distance between sample and the ICP plasma tube above 120 mm, and a good passivation quality on a flat as well as on a textured front surface.

The a-Si:H(i) layers deposited by PP PECVD technology have a quite high initial growth rate, a constant optical energy band gap regarding the a-Si:H(i) layer thickness, a very good homogeneity which is independent of the distance between the parallel plates, and an excellent passivation quality on flat as well as on a textured front surface.

A comparison of the a-Si:H(i) layers deposited by ICP and PP PECVD in a SHJ solar cells batch including a variation of the a-Si:H(i) and a-Si:H(p) layer thickness revealed no significant differences. The best solar cells produced within this investigation were: η_{ICP}=18.7% (confirmed by ISE CalLab) and η_{PP}=18.6%.

ACKNOWLEDGEMENT

The authors would like to thank S. Seitz, T. Leimenstoll, A. Stifel, I. Druschke, F. Schaetzle, A. Filipovic, and E. Schäffer for process technology and measurements. The work has been supported by the German Federal Ministry for the Environment, Nature Conservation and Nuclear Safety under contract number 0329849A „Th-ETA“.

REFERENCES

[1] T. Mueller, S. Schwertheim, and W. R. Fahrner, "Application of wide-bandgap hydrogenated amorphous silicon oxide layers to heterojunction solar cells for high quality passivation," presented at Proceedings of the 33rd IEEE Photovoltaic Specialists Conference, San Diego, CA, USA, 2008.

[2] L. Korte, E. Conrad, H. Angermann, R. Stangl, and M. Schmidt, "Overview on a-Si:H/c-Si heterojunction solar cells - physics and technology," presented at Proceedings of the 22nd European Photovoltaic Solar Energy Conference, Milan, Italy, 2007.

[3] S. Olibet, C. Monachon, A. Hessler-Wyser, E. Vallat-Sauvain, S. De Wolf, L. Fesquet, J. Damon-Lacoste, and C. Ballif, "Textured silicon heterojunction solar cells with over 700 mV open-circuit voltage studied by transmission electron microscopy," presented at Proceedings of the 23rd European Photovoltaic Solar Energy Conference, Valencia, Spain, 2008.

[4] E. Maruyama, A. Terakawa, M. Taguchi, Y. Yoshimine, D. Ide, T. Baba, M. Shima, H. Sakata, and M. Tanaka, "Sanyo´s challenges to the development of high-efficiency HIT solar cells and the expansion of HIT business," presented at Proceedings of the 4th World Conference on Photovoltaic Energy Conversion, Waikoloa, Hawaii, USA, 2006.

[5] H. Fujiwara and M. Kondo, "Effects of a-Si:H layer thicknesses on the performance of a-Si:H/c-Si heterojunction solar cells," *Journal of Applied Physics*, vol. 101, pp. 054516/1-9, 2007.

[6] Q. Wang, M. R. Page, E. Iwaniczko, Y. Q. Xu, L. Roybal, R. Bauer, B. To, H. C. Yuan, A. Duda, and Y. F. Yan, "Crystal silicon heterojunction solar cells by hot-wire CVD," presented at Proceedings of the 33rd IEEE Photovoltaic Specialists Conference, San Diego, CA, USA, 2008.

[7] M. Edwards, S. Bowden, U. Das, and M. Burrows, "Effect of texturing and surface preparation on lifetime and cell performance in heterojunction silicon solar cells," *Solar Energy Materials and Solar Cells*, 2008.

[8] D. Pysch, J. Ziegler, J.-P. Becker, D. Suwito, S. Janz, S. W. Glunz, and M. Hermle, "Stretched-exponential increase in the open-circuit voltage induced by thermal annealing of amorphous silicon-carbide heterojunction solar cells," *Applied Physics Letters*, vol. 94, pp. 093510/1-3, 2009.

[9] M. Taguchi, Y. Tsunomura, H. Inoue, S. Taira, T. Nakashima, T. Baba, H. Sakata, and E. Maruyama, "High-efficiency HIT solar cell on thin (<100µm) silicon wafer," presented at Proceedings of the 24th European Photovoltaic Solar Energy Conference, Hamburg, Germany, 2009.

[10] T. Sawada, N. Terada, S. Tsuge, T. Baba, T. Takahama, K. Wakisaka, S. Tsuda, and S. Nakano, "High-efficiency a-Si/c-Si heterojunction solar cell," presented at Proceedings of the 1st World Conference on Photovoltaic Energy Conversion Hawaii, USA, 1994.

[11] S. Taira, Y. Yoshimine, T. Baba, M. Taguchi, H. Kanno, T. Kinoshita, H. Sakata, E. Maruyama, and M. Tanaka, "Our approaches for achieving hit solar cells with more than 23% efficiency," presented at Proceedings of the 22nd European Photovoltaic Solar Energy Conference Milan, Italy, 2007.

[12] D. Pysch, M. Bivour, K. Zimmermann, C. Schetter, M. Hermle, and S. W. Glunz "Comprehensive study of different PECVD-deposition methods for deposition of thin intrinsic amorphous silicon for heterojunction solar cells," presented at Proceedings of the 24th European Photovoltaic Solar Energy Conference, Hamburg, Germany, 2009.

[13] A. Richter, J. Benick, and S. W. Glunz, "Spectral ellipsometry analysis of ultrathin amorphous silicon layers," presented at Proceedings of the 23rd European Photovoltaic Solar Energy Conference, Valencia, Spain, 2008.

[14] R. A. Sinton and A. Cuevas, "A quasi-steady-state open-circuit voltage method for solar cell characterization," presented at Proceedings of the 16th European Photovoltaic Solar Energy Conference, Glasgow, UK, 2000.

[15] H. Angermann, J. Rappich, and C. Klimm, "Wet-chemical treatment and electronic interface properties of silicon solar cell substrates " *Central European Journal of Physics*, vol. 7, pp. 363-70, 2009.

[16] J.-P. Becker, D. Pysch, A. Leimenstoll, M. Hermle, and S. W. Glunz "Wet-chemical pre-treatment of c-Si substrates enhancing the performance of a-SiC:H/c-Si heterojunction solar cells," presented at Proceedings of the 24th European Photovoltaic Solar Energy Conference, Hamburg, Germany, 2009.

[17] A. Mette, C. Schetter, D. Wissen, S. Lust, S. W. Glunz, and G. Willeke, "Increasing the efficiency of screen-printed silicon solar cells by light-induced silver plating," presented at Proceedings of the 4th World Conference on Photovoltaic Energy Conversion, Waikoloa, Hawaii, USA, 2006.

[18] M. A. Lieberman and A. J. Lichtenberg, *Principles of plasma discharges and materials processing*: John Wiley & Sons, Inc. , 1994.

[19] Y. Takeuchi, I. Kawasaki, H. Mashima, M. Murata, and Y. Kawai, "Characteristics of VHF excited hydrogen plasmas using a ladder-shaped electrode," *Thin Solid Films*, vol. 390, 2001.

[20] S. J. Schreiber, "Plasma deposition of microcrystalline silicon for thin film transistors," in *Department of Engineering*. Cambridge: University of Cambridge, 2001, pp. 177.

[21] S. K. Kim, Y. J. Choi, K. S. Cho, and J. Jang, "Hydrogen dilution effect on the properties of coplanar amorphous silicon thin-film transistors fabricated by inductively-coupled plasma CVD," *IEEE Transactions on Electron Devices*, vol. 46, pp. 1001-6, 1999.

[22] M. Jeon, K. Kawachi, P. Supajariyawichai, M. Dharmrin, and K. Kamisako, "Characterization of the intrinsic amorphous silicon (a-Si:H) layer prepared by remote-PECVD for heterojunction solar cells: effect of the annealing treatment on multi-crystalline Si wafer," *e-Journal of Surface Science and Nanotechnology*, vol. 6, pp. 124-9, 2008.

[23] J. Robertson, "Electronic structure of silicon nitride," *Philosophical Magazine B (Physics of Condensed Matter*, vol. 63, pp. 47- 77, 1991.

[24] J. Robertson, "Defects and hydrogen in amorphous silicon nitride," *Philosophical Magazine B (Physics of Condensed Matter, Electronic, Optical and Magnetic Properties)*, vol. 69, pp. 307- 26, 1994.